2014

A Neural Network to Predict the Temperature Distribution in Hermetic Refrigeration Compressors

Ernane Silva
POLO / UFSC, Brazil, ernane@polo.ufsc.br

Marco C. Diniz
POLO / UFSC, Brazil, marcodiniz@polo.ufsc.br

Cesar J. Deschamps
POLO / UFSC, Brazil, deschamps@polo.ufsc.br

A Neural Network to Predict the Temperature Distribution in Hermetic Refrigeration Compressors

Ernane SILVA, Marco C. DINIZ, Cesar J. DESCHAMPS*

POLO Research Laboratories for Emerging Technologies in Cooling and Thermophysics
Federal University of Santa Catarina
Florianópolis, SC, Brazil
deschamps@polo.ufsc.br

* Corresponding Author

ABSTRACT

The understanding of heat transfer interactions in refrigeration compressors is of fundamental importance to characterize their overall performance. Certain temperatures, such as those of the motor, oil, shell, and at suction and discharge chambers, have strong influence on the compressor electrical consumption and reliability. Experimental and numerical approaches have been successfully employed to characterize the thermal profile of compressors under different operating conditions. This paper presents a multi-layered feed-forward neural network developed to predict the main temperatures of a hermetic reciprocating compressor. Such a model can be used for different compressor layouts without major modifications, being a fast method for estimating temperatures without the solution of the compression cycle. Predictions of the neural network were compared with experimental data and numerical results from comprehensive thermodynamic simulations, and good agreement was observed in a wide range of evaporating and condensing temperatures. The neural network was found to predict the temperature distribution with sufficient accuracy for compressor analysis and development.

1. INTRODUCTION

The characterization of heat transfer between the components of hermetic reciprocating compressors is necessary in a detailed analysis of compressor performance. Aspects such as the increase of gas temperature during the suction process act to reduce the system cooling capacity and to increase power consumption. Moreover, it is important to monitor temperature of different components, such as motor, oil and shell, due to reliability issues.

Although difficult to predict (Prasad, 1998), the phenomena involving heat transfer in hermetic compressors has captured the attention of several researchers in the last twenty years. In this context, several numerical approaches with different degrees of complexity have been employed to estimate the temperature field in hermetic compressors. Predictions of the temperature field are usually associated with the simulation of the compression cycle. For instance, Todescat *et al.* (1992) developed a semi-empirical model to characterize the compression cycle and the compressor temperature distribution, by using measurements to establish thermal conductances between different components. The authors observed good agreement between numerical and experimental results. In order to avoid the necessity of measurements for calibration purposes, Ooi (2003) developed a thermal network model (TNW) in which thermal resistances between components were represented through classic heat transfer correlations available in the literature. Results indicated that, although more flexible than the model proposed by Todescat *et al.* (1992), the TNW model is highly dependent on the availability of adequate heat transfer correlations.

More recently, complex models such as the fully CFD model developed by Birari *et al.* (2006) and the hybrid models proposed by Ribas *et al.* (2007) and Sanvezzo *et al.* (2012) have been employed to analyze heat transfer in hermetic compressors. Although accurate, these models require high computational resources and are not useful when fast calculations of the temperature field are necessary.

Artificial neural networks are able to reproduce existing relationships between inputs and outputs of highly non-linear systems and have been used for many purposes, from curve fitting to robot vision and speech recognition. Neural networks have also been employed in the thermodynamic modeling of compressors. Yang *et al*. (2009), for example, developed a loss-efficiency model to predict volumetric and isentropic efficiencies for positive displacement compressors using neural networks. Compression ratio, condensing temperature and evaporating temperature were used as input parameters and with one more input parameter, frequency, they were able to extend the model to variable speed compressors. Standard deviations smaller than 0.4% and errors falling within ±1.3% were observed when comparing predictions with manufacturer data. Also, Sanaye *et al*. (2011) predicted the mass flow rate and discharge temperature of a rotary vane compressor with a neural network. Suction temperature and pressure as well as compressor speed and discharge pressure were the inputs. The network was able to fit the experimental data with a correlation coefficient in the range of 0.962-0.998 and mean relative errors in the range of 2.79-7.36%. Neural networks have also been employed to predict performance maps for axial compressors based on manufacturer data (Yu *et al*., 2007; Ghorbanian and Gholamrezaei, 2009).

Although the literature review reveals no artificial neural networks for thermal analysis of compressors, we consider this method as an alternative and viable approach. In this paper we report an artificial neural network developed to predict the temperatures at different locations in a reciprocating compressor for different condensing and evaporating temperatures. The experimental procedure and setup used to obtain data for the neural network is described next, followed by the detailed explanation of the neural network. The results obtained with the neural network are compared with experimental data and with predictions of a simulation model based on the approach of Todescat et al. (1992).

2. EXPERIMENTAL PROCEDURE

The neural network developed in this work requires experimental data for training. For this reason, a small hermetic reciprocating compressor was instrumented and tested in a hot-cycle test bench. The compressor instrumentation and the procedure followed in the tests are described in this section.

2.1 Compressor instrumentation

The temperatures in different locations of the compressor were measured with thermocouples. Measurements of the refrigerant were carried out in the suction line (T_{in}), suction muffler inlet ($T_{suc,2}$), suction muffler outlet ($T_{suc,1}$), discharge environment ($T_{dis,1}$), discharge muffler ($T_{dis,2}$), discharge line (T_{out}) and compressor internal environment (T_{ie}). The temperature of solid components was also monitored thorough thermocouples in the cylinder wall (T_w), motor coil (T_{coil}), motor stator (T_{sta}) and compressor shell (T_{shell}). The temperature of the lubricant oil was measured with a sensor positioned in the oil sump (T_{oil}). A schematic view of the compressor employed in the tests and the positions where the thermocouples were instrumented are given in Figure 1.

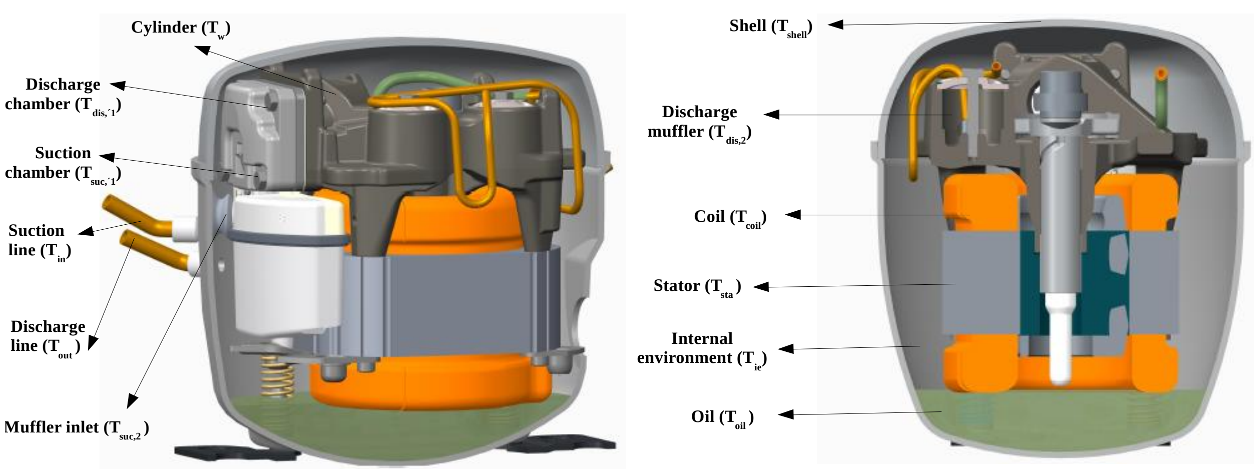

Figure 1: Compressor instrumentation

2.2 Experimental Setup

The instrumented compressor was tested in a hot-cycle test bench widely used for compressor testing. In this test facility, the compressor is submitted to a pressure ratio controlled by valves and a suction line temperature obtained through heat exchangers. In the hot-cycle test bench, all the thermodynamic processes occur with the gas in the superheated vapor state. Therefore, phase change is avoided and quick compressor tests can be obtained. Details about the operation of such a test bench are available in Dutra and Deschamps (2013).

A total of 16 tests were conducted to evaluate the compressor temperature field and calibrate the artificial neural network, by combing four evaporating temperatures (-25ºC, -20ºC, -15ºC and -10ºC) and four condensing temperatures (45ºC, 50ºC, 55ºC and 60ºC). Each test was performed just once. Measurement repeatability was assessed by testing the compressor five times in the reference condition represented by the evaporating temperature of -23.3ºC and condensing temperature of 54.4ºC. These five testes were randomly carried out between aforementioned the calibration tests. The tests were stopped when the compressor was considered thermally stabilized. This condition was achieved when during 30 minutes all the temperatures presented a maximum variation of ± 0.5˚C. Then, the next 30 minutes in the test were used to calculate an average temperature. Table 1 presents the results obtained for the reference condition.

The performance of the neural network was assessed by comparing its predictions with experimental data not used in the network training. In this respect, four random tests were used to validate the neural network following the operating conditions shown in table 2.

Table 1: Experimental results for the reference condition

Condition [ºC]	**Performance**	**Temperatures [ºC]**					
-23.3 / 54.4	**Mass Flux [kg/h]**	T_{in}	$T_{suc,2}$	$T_{suc,1}$	$T_{dis,1}$	$T_{dis,2}$	T_{out}
	4.75 kg/h	35.6	43.6	56.3	133.9	110.6	89.6
	Consumption [W]	T_{ie}	T_{w}	T_{coil}	T_{sta}	T_{shell}	T_{oil}
	144.5 W	84.9	95.9	88.5	87.7	76.9	74.8

Table 2: Validation tests operating conditions

Reference name	**Evaporating temperature [ºC]**	**Condensing temperature [ºC]**
Val 1	-17.0	47.9
Val 2	-21.8	57.5
Val 3	-19.0	54.0
Val 4	-14.6	52.0

3. NEURAL NETWORK

The neural network used was developed in the MATLAB environment, more specifically with Neural Network Toolbox (Beale *et al*., 2012). It can be considered a feed-forward network, that is, the output of each layer can be used as inputs for the next layers only, never for the same layer or previous layers. Evaporating and condensing temperatures, T_C and T_E, are provided as the inputs and temperatures at different locations of the compressor are expected as outputs, T_1 to T_K. Figure 2 presents a schematic view of the neural network, where each circle represents a neuron or processing unit and the arrows represent network connections.

As depicted in Figure 2, the network consists of two layers: a hidden layer with a sigmoid transfer function and an output layer with a linear transfer function. According to Kröse and van der Smagt (1996), only one hidden layer suffices to approximate any function with finitely many discontinuities to arbitrary precision, provided the transfer function of this layer is non-linear, which is the case of the sigmoid function.

In each neuron the following operations are carried out:

(a) the net input, *s*, for each neuron is calculated as

$$s = \sum_{i=1}^{N} w_i p_i + \theta$$

where p_i are the outputs from the previous layer and w_i are their respective weights. Θ is simply and additive constant, the bias.

(b) the neuron output, *y*, is calculated according to:

$$y = f(s)$$

where *f* is the transfer function.

With the network defined, the values of the weights and biases must be found in order to properly model the phenomenon of interest. This is done by means of a training algorithm and previous known data from the process (samples). The training algorithm performs the minimization of the difference between the network outputs and the targets (samples outputs) with the weights and biases as the optimization variables. When the optimum parameters are found it is expected that the neural network would be able to make correct predictions about the phenomenon. The samples used for the network training were described in section 2.2. Two training algorithms were evaluated: Levenberg-Marquardt and Bayesian regularization.

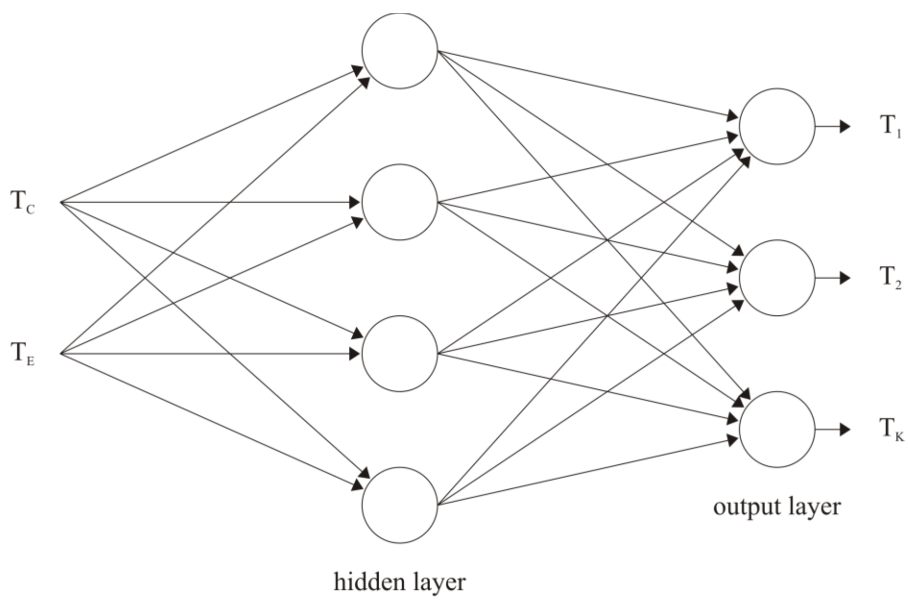

Figure 2: Neural network scheme.

4. RESULTS

4.1 Neural Network Training

The neural network is composed of two inputs, namely, the condensing and evaporating temperatures, and twelve outputs, that is, all temperatures monitored experimentally, as described in section 2. Eight neurons were employed in the hidden layer. As a first attempt, the Levenberg-Marquardt training algorithm was used, but it was very difficult to converge. Therefore, the Bayesian regularization was used instead and showed to be more stable. With this training algorithm a correlation factor above 0.99 was obtained in fitting the experimental data (Figure 3).

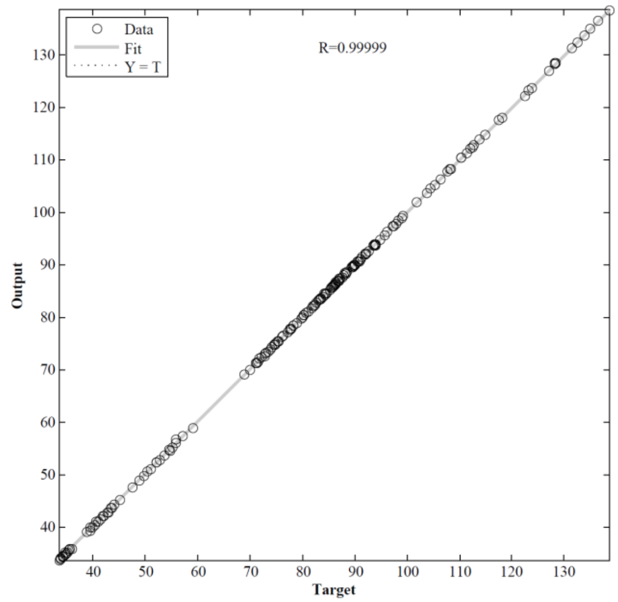

Figure 3: Regression of experimental data

4.2 Validation

To evaluate the applicability of the neural network model (NN), the results obtained were compared to experimental data and to predictions of an available numerical model, hereafter denominated physical model (PM).

This physical model is based on the model developed by Todescat et al. (1992) and simulates the compression cycle using a transient lumped formulation for the conservation equations. The volume inside the compression chamber is estimated from geometrical parameters, and models for the mass flow rate and valve dynamics are also considered. This model has been successfully employed in a variety of operating conditions. Heat transfer between different components inside the compressor is modeled with a lumped formulation of the energy equation. The components thermally interact with each other through global heat conductances obtained experimentally. In this work, the necessary global heat transfer conductances were obtained with the experimental data for the reference condition (Table 1). Such heat transfer conductances were used in all simulations of the present study.

Table 3 presents temperatures predicted by the trained neural network (NN) and the physical model (PM) as well as the experimental results (ER) for the randomly selected validation conditions. Absolute deviation between predictions and experimental data is written in italic. It should be mentioned that not all temperatures indicated in Table 3 can be predicted by the physical model.

As can be seen, all temperatures predicted by the neural network are within 1ºC of difference in relation to the experimental data, with the highest deviations being observed for the suction muffler outlet ($T_{suc,1}$) and oil (T_{oil}) temperatures. Good agreement with experimental data is also verified for predictions provided by the PM, but the results of the NN are in better agreement for most of the operating conditions. However, it must be noticed that the PM requires only one experimental test for calibration. The smallest deviation verified for the PM model occurs in the Val 2 test, which is an operating condition close to the condition used for its calibration.

Table 3: Comparison between experimental and simulated data

Temperature (°C)												
Model		**$T_{suc,2}$**	**$T_{suc,1}$**	**T_w**	**$T_{dis,1}$**	**$T_{dis,2}$**	**T_{out}**	**T_{oil}**	**T_{ie}**	**T_{coil}**	**T_{sta}**	**T_{shell}**
1	ER	41.1	51.7	90.0	123.8	106.0	89.2	72.4	82.3	85.6	84.3	74.5
	NN	40.7 *-0.4*	51.6 *-0.1*	89.6 *-0.4*	123.5 *-0.3*	105.6 *-0.4*	89.2 *0.0*	71.6 *-0.8*	82.0 *-0.3*	85.2 *-0.4*	83.8 *-0.5*	74.1 *-0.4*
	PM	-	49.2 *-2.5*	88.3 *-1.7*	120.2 *-3.6*	106.7 *+0.7*	90.6 *+1.4*	-	81.3 *-1.0*	85.8 *+0.2*	-	73.9 *-0.6*
2	ER	44.1	56.0	97.5	136.0	112.6	92.3	75.8	86.7	90.3	89.3	78.3
	NN	43.8 *-0.3*	56.8 *+0.8*	97.3 *-0.2*	135.3 *-0.7*	112.1 *-0.5*	91.4 *-0.9*	76.2 *+0.4*	86.6 *-0.1*	90.3 0.0	89.5 +0.2	78.4 *+0.1*
	PM	-	55.7 *-0.3*	96.5 *-1.0*	135.0 *-1.0*	113.2 *+0.6*	92.3 *0.0*	-	86.4 *-0.3*	90.1 *-0.2*	-	78.2 *-0.1*
3	ER	42.2	53.7	94.2	130.1	109.8	91.5	75.0	85.2	89.0	87.7	77.1
	NN	42.3 *-0.1*	54.4 *+0.7*	94.7 *+0.5*	131.0 *+0.9*	110.7 *+0.9*	92.1 *+0.6*	75.0 *0.0*	85.7 *+0.5*	89.2 *+0.2*	88.1 *+0.4*	77.4 *+0.3*
	PM	-	51.4 *-2.3*	93.2 *-1.0*	129.3 *-0.8*	112.0 *+2.2*	93.0 *+1.5*	-	84.7 *-0.5*	88.9 *-0.1*	-	76.8 *-0.3*
4	ER	40.7	52.2	91.5	125.4	108.0	92.3	74.0	84.6	88.1	86.5	76.3
	NN	40.5 *-0.2*	51.6 *-0.6*	91.1 *-0.4*	125.2 *-0.2*	107.8 *-0.2*	92.0 *-0.3*	73.2 *-0.8*	84.0 *-0.6*	87.5 *-0.6*	85.8 *-0.7*	75.8 *-0.5*
	PM	-	57.7 *-4.6*	88.9 *-2.6*	121.8 *-3.7*	109.5 *+1.5*	94.0 *+1.7*	-	83.0 *-1.6*	88.1 *0.0*	-	75.3 *-1.0*

4.3 Influence of pressure ratio

In a typical refrigeration cycle, pressure ratio variation occurs due to variation in the operating conditions, especially the thermal load. Therefore, it is important to quantify the variation of compressor temperatures in these conditions.

Figure 4 presents the comparison between numerical and experimental results of compressor temperatures for several condensing temperature and evaporating temperature of -25ºC. Despite the fact that the results obtained by the neural network present greater agreement with experimental data, it is important to notice that the physical model (PM) is also capable of representing the trends observed in the experimental data.

The comparison between Figures 4(a) and 4(b) indicates that the discharge temperature is increased to a greater extent than the suction temperature as the pressure ratio increases. Nevertheless, Figures 4(c) and 4(d) show that the difference between the temperatures of shell (T_{shell}) and internal environment (T_{ie}) and between the temperatures of cylinder wall (T_w) and coil (T_{coil}) remain approximately constant as the pressure ratio increases.

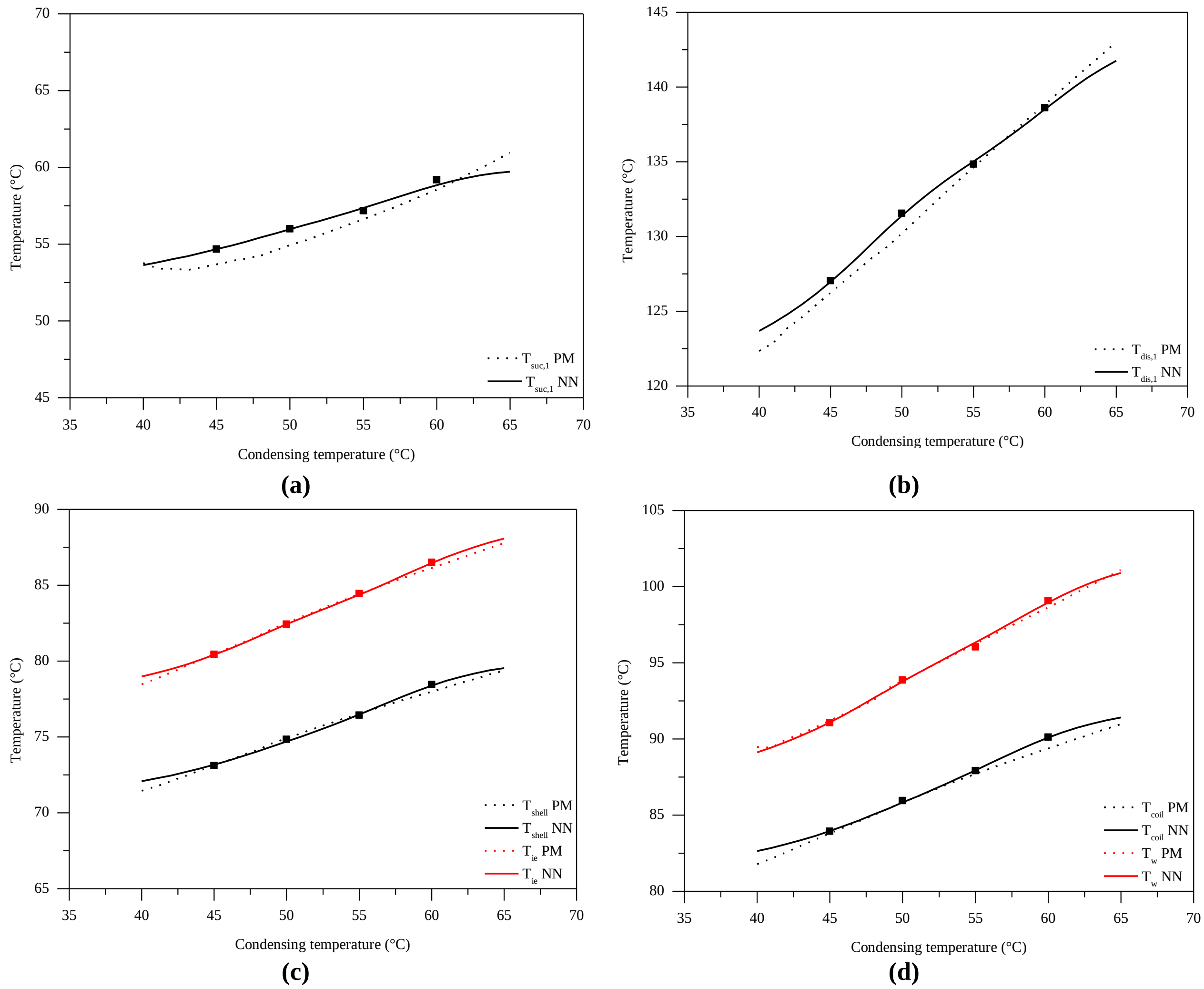

Figure 4: Comparison of NN, PM and experimental data for T_e = -25 ºC.

Figure 5 presents the comparison between numerical and experimental results of compressor temperatures for several condensing temperature and evaporating temperature of -10ºC. The neural network was found to adequately predict the temperatures variation with pressure ratio. On the other hand, the physical model (PM) could not predict the temperatures with the same accuracy observed for the evaporating temperature of -25ºC, probably because the global heat conductances adopted in the model were obtained for the reference condition (-23.3/54.4). In this operating condition, the neural network presents significant better predictions than the physical model. Therefore, considering its simplicity and accuracy, the neural network represents a viable alternative to predict the thermal profile of compressors.

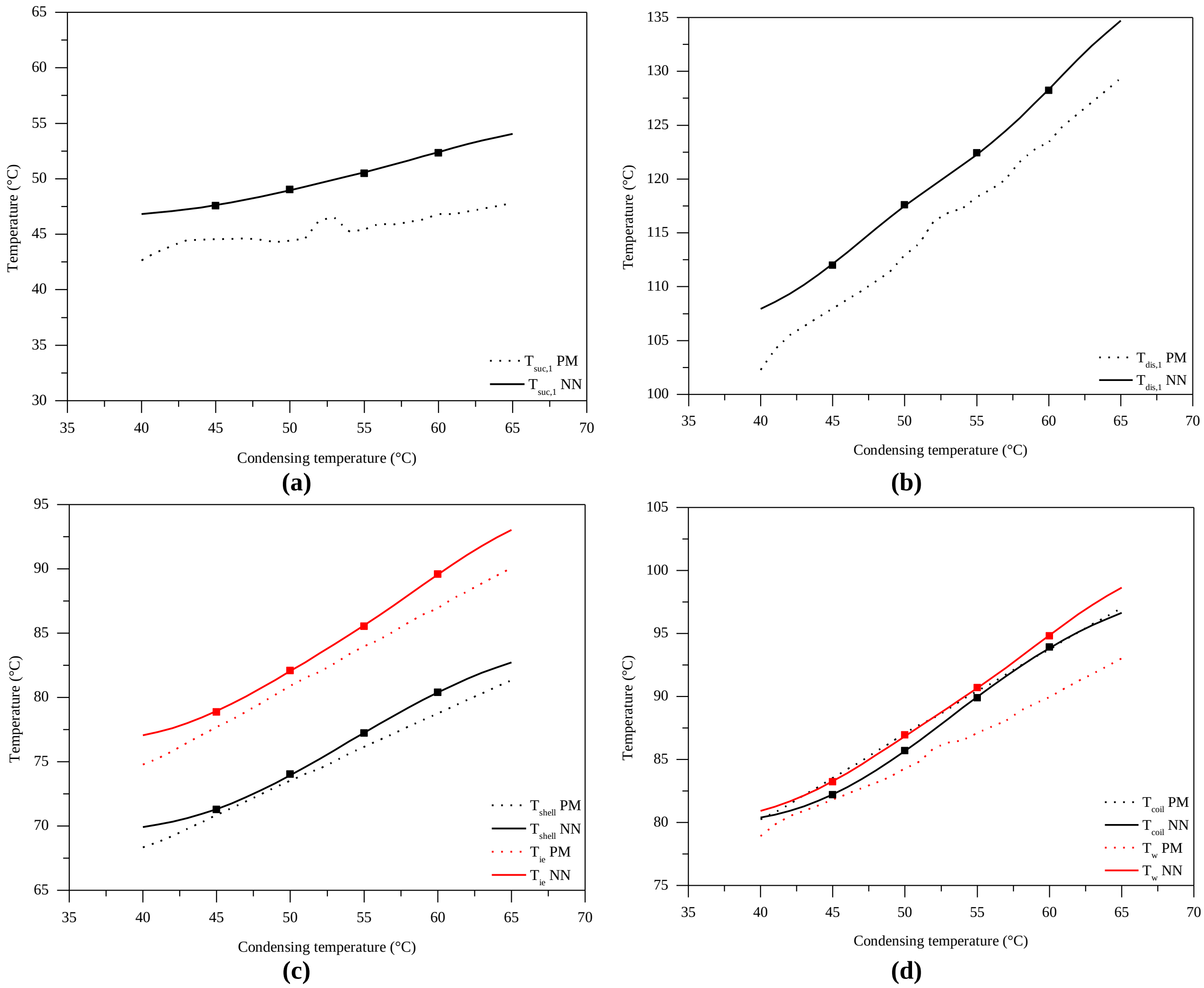

Figure 5: Comparison of NN, PM and experimental data for T_e = -10ºC.

5. CONCLUSIONS

The present work reported a neural network developed to predict the temperature distribution in a reciprocating compressor adopted for household refrigeration. Experimental data for 16 tests were used to train the neural network, and the results obtained were validated using 4 random tests. A physical model was also included in the analysis for comparison purposes. It was observed that the physical model predicts temperatures in excellent agreement with experimental data only when the operating condition is similar to that of its calibration test. On the other hand, the neural network was able to correctly characterize the compressor temperature distribution in all conditions analyzed. The neural network is found to be a valid alternative to predict the temperature distribution of compressor prototypes subjected to different operating conditions. Besides its simplicity, this method provides fast results with excellent accuracy.

NOMENCLATURE

General and Greek symbols

p	Layer output	( )	s	Net input	( )
T	Temperature	(ºC)	w	Output weights	( )

T_e	Evaporation temperature	(°C)	y	Neural network output	( )
T_c	Condensation temperature	(°C)	θ	Bias	( )

Subscripts

coil	Motor coil	out	Compressor outlet
dis,1	Discharge environment	shell	Compressor shell
dis,2	Discharge muffler	sta	Motor stator
ie	Internal environment	suc,1	Suction muffler outlet
in	Suction line	suc,2	Suction muffler inlet
oil	Lubricant oil	w	Cylinder wall

REFERENCES

Beale, M.H., Hagan, M.T., Demuth, H.B., 2012, *Neural Network Toolbox User's Guide*, Mathworks Inc., Natick, 420 p.

Birari, Y.V, Gosavi, S.S, Jorwekar, P.P, 2006, Use of CFD in Design and Development of R404a Reciprocating Compressor, Proc. Int. Compressor Engrg. Conf. at Purdue, Paper C072.

Dutra, T., Deschamps, C.J., 2013, "Experimental characterization of heat transfer in the components of a small hermetic reciprocating compressor", *Appl. Thermal Engineering*., vol. 58, p. 499-510.

Ghorbanian, K., Gholamrezaei, M., 2009, An artificial neural network approach to compressor performance prediction, *Appl. Energ.*, vol. 86, no. 7-8: p. 1210-1221.

Kröse, B., van der Smagt, P., 1996, *An Introduction to Neural Networks*, Amsterdam, 130 p.

Ooi, K.T., 2003, Heat Transfer Study of a Hermetic Refrigeration Compressor, Applied Thermal Engineering, v.23 pp. 1931–1945.

Ribas Jr., F.A., 2007, Thermal Analysis of Reciprocating Compressors, Proc. Int. Conf. on Compressors and Their Systems, London, pp. 277-287.

Sanaye, S., Dehghandokht, M., Mohammadbeigi, H., Bahrami, S., 2011, Modeling of rotary vane compressor applying artificial neural network, *Int. J. Refrig.*, vol. 34, no. 3: p. 764-772.

Shiva Prasad, B.G., 1998, Heat Transfer in Reciprocating Compressors - A Review, Proc. Int. Compressor Engrg. Conf. at Purdue, pp. 857-863.

Sanvezzo Jr, Joel and Deschamps, Cesar J., 2012, "A Heat Transfer Model Combining Differential and Integral Formulations for Thermal Analysis of Reciprocating Compressors", Proc. Int. Compressor Engrg. Conf. at Purdue, Paper 2104.

Todescat, M.L., Fagotti, F., Prata, A.T., Ferreira, R.T.S., 1992, Thermal Energy Analysis in Reciprocating Hermetic Compressors, Proc. Int. Compressor Engrg. Conf. at Purdue, pp. 1417-1428.

Yang, L., Zhao, L.X., Zhang, C.L., Gua, B., 2009, Loss-efficiency model of single and variable-speed compressors using neural networks, *Int. J. Refrig.*, vol. 32, no. 6: p. 1423-1432.

Yu, Y., Chen, L., Sun, F., Wu, C., 2007, Neural-network based analysis and prediction of a compressor's characteristic performance map, *Appl. Energ.*, vol. 84, no. 1: p. 48-55.

ACKNOWLEDGEMENTS

The present study was developed as part of a technical-scientific cooperation program between the Federal University of Santa Catarina and EMBRACO. The authors also thank the support of CNPq (National Council of Research) through grant 573581/2008-8 (National Institute of Science and Technology in Refrigeration and Thermo physics).